ANTIOXIDANTS & REDOX SIGNALING
Volume 8, Numbers 5 & 6, 2006

Forum Original Research Communication

Role of the Cytosolic Loop of DsbB in Catalytic Turnover of the Ubiquinone–DsbB Complex

YOH-HEI TAKAHASHI, KENJI INABA, and KOREAKI ITO

ABSTRACT

DsbB, an *Escherichia coli* plasma membrane protein, oxidizes DsbA, the protein dithiol oxidant in the periplasm, in conjunction with respiratory quinone molecules. While its two periplasmic regions, in particular the essential Cys41–Cys44 and the Cys104–Cys130 cysteine pairs, have been characterized in considerable detail, little or no information is available about the functional importance of its three cytosolically disposed regions. In this work the authors introduced insertion and substitution mutations into the short (~6 residue) central cytosolic loop. The purified mutant proteins proved to have two of the essential cysteines reduced and to exhibit the spectroscopic transition of bound ubiquinone constitutively. A thrombin-cleavage site present in a mutant protein called DsbB-T established that the mutant protein had a rearranged Cys41–Cys130 disulfide that would unpair Cys44. Although this covalent structure of DsbB is reminiscent of the DsbB–DsbA intermediate, in which unpaired Cys44 induces the ubiquinone transition, it is inactive because of the premature disulfide rearrangement without involving DsbA. In addition, ubiquione-mediated *in vitro* oxidation of reduced DsbB-T was aborted at a half-oxidized state, without rapidly producing the fully oxidized enzyme. Thus, the cytosolic loop alterations compromised the catalytic turnover of DsbB *in vitro*. These observations suggest that the cytosolic loop is important to coordinate the active-site residues of DsbB and ubiquinone to allow their proper reaction cycles. *Antioxid. Redox Signal.* 8, 743–752.

INTRODUCTION

The Dsb enzymes in the periplasmic space and the plasma membrane of *Escherichia coli* function in the formation of correctly positioned disulfide bonds in the cell-surface localized proteins (11, 15). The primary dithiol oxidant in the periplasm, DsbA, donates its active site disulfide (Cys30–Cys33) to proteins that are exported from the cytosol. The DsbA disulfide bond is then restored by a membrane protein DsbB that utilizes the oxidizing power of respiratory quinones, ubiquinone (UQ) in aerobiosis or menaquinone in anaerobiosis (1, 3, 7, 13, 19). DsbB traverses the membrane four times, forming two functionally important periplasmic regions. Its N and C termini as well as the central loop are localized on the cytosolic side of the membrane. Each of the first and the second periplasmic domain contains a pair of essential cysteines, Cys41–Cys44 and Cys104– Cys130, respectively, in the forms of disulfides (9; Fig. 1a). The latter is believed to interact directly with the DsbA cysteines (5, 12) and the former to interact with quinones (1, 3, 14).

In recent years, different views have been put forward about reactivities and roles of the DsbB cysteines and of the bound UQ in the DsbA oxidation catalysis (4, 6–8, 10, 16, 17, 19). Here, we summarize our own views obtained from a series of detailed analyses we have conducted on the DsbB- and quinone-dependent oxidation of DsbA (6–8, 19). Our analyses using quinone-bearing and quinone-free forms of DsbB indicate that both of its cysteine pairs have significantly lower redox potentials than the DsbA cysteines. Despite this apparent paradox, oxidized DsbB can react with reduced DsbA in two alternative ways.

Institute for Virus Research, Kyoto University and CREST, Japan Science and Technology Agency, Kyoto, Japan.

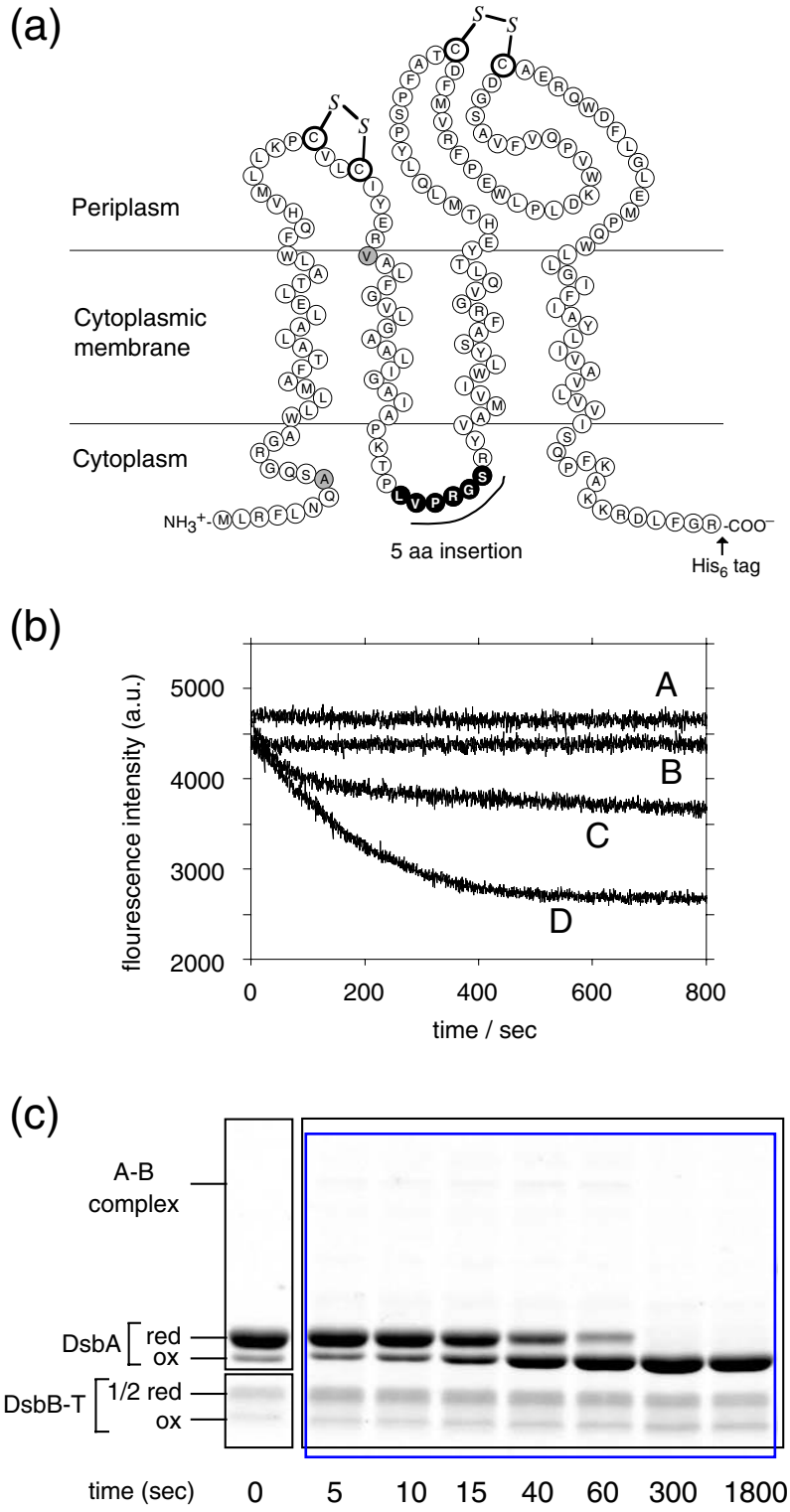

FIG. 1. DsbB-T is functionally defective. (**a**) Primary structure and possible arrangement of DsbB-T in the membrane. A thrombin-cleavable Leu–Val– Pro–Arg–Gly–Ser sequence (*solid circles*) was introduced into the cytosolic loop. Ala at position 8 and Val at position 49 are shown in *gray* to indicate that they replaced the nonessential Cys residues at these positions. (**b**) Impaired DsbA oxidation catalysis by DsbB-T. Oxidation-dependent decrease of DsbA (10 μ*M*) fluorescence intensity was followed in the absence (B) or the presence of a catalytic amount (10 n*M*) of wild-type DsbB (D) or DsbB-T (A) and of 200 n*M* DsbB-T (C). Reactions were all in the presence of externally added UQ1 (10 μ*M*). (**c**) Equimolar reaction between reduced DsbA and DsbB-T. Reduced DsbA and DsbB-T (10 μ*M* each) were mixed in the presence of UQ1 (200 μ*M*). Redox state changes of DsbA and DsbB-T were followed by samplings at the indicated time points into TCA and following AMS modification and SDS-PAGE, as described in Materials and Methods.

In the first pathway, rapid thiol–disulfide exchange occurs between the DsbA cysteines (Cys30 and Cys33) and the Cys104–Cys130 DsbB disulfide, followed by immediate thiol–disulfide equilibrium within DsbB, between the Cys41/Cys44 and the Cys104/Cys130 pairs, producing two hemioxidized forms of DsbB. In the normal quinone-coupled reaction, the Cys41/Cys44 pair is oxidized by UQ or menaquinone leading to the regeneration of fully oxidized DsbB and production of reduced quinols, the latter of which is then recycled back by terminal oxidases.

In the second pathway, the initial formation of an intermediate disulfide between Cys30 (DsbA) and Cys104 (DsbB) is

followed by the formation of the rearranged Cys41–Cys130 disulfide bond within DsbB (7, 8, 10, 19). This binary complex is stable in the absence of quinones, but normally it is resolved slowly into oxidized DsbA, oxidized DsbB, and reduced quinols. A striking feature in the second (slow) pathway is that unpaired Cys44 in the binary complex somehow induces a spectroscopic transition (red shift) of bound quinones (7, 19). Thus, UQ on the intermediate develops pink color with absorption peak at ~500 nm, whereas menaquinone develops violet color with absorption peak at ~550 nm. The importance of thiolate anions of Cys44 in the spectroscopic transition of quinones has been shown by the following observations (7). First, serine substitutions for some cysteine residues with expected outcome of Cys44 reduction cause the quinone transition constitutively without involving DsbA. Second, a cysteine-alkylating agent acts to abolish the transition. Finally, the transition is pH-dependent, showing apparent pK_a value of ~6.6 for the transition. The spectroscopic transition of quinone appears to occur during the first pathway as well, albeit very briefly (7, 19).

Regeimbal *et al*. (17) also described a 500-nm absorption for DsbB. Unlike our observations, they noted marked absorption spectrum in their DsbB preparations without involving DsbA or any mutational alterations. They proposed that UQ on DsbB forms a quinhydrone-like charge-transfer complex with hydroquinone molecules that are constitutively associated with DsbB. However, we observed the same spectral change with quinone-free DsbB prepared from mutant cells incapable of synthesizing any quinone molecule, when it was supplemented with DsbA (C33S) and UQ, making the contribution by hydroquinone unlikely. Thus, our conclusions and those of Regeimbal *et al*. are significantly different in important issues: (a) whether the transition is induced by unpaired Cys44 or it is a constitutive trait of DsbB, and (b) whether hydoroquinone is involved.

In this study, we found that alterations of the short cytosolic loop of DsbB cause constitutive UQ transition, at least after purification of the variant proteins. In the mutant proteins, DsbB cysteines are partially reduced such that Cys41 and Cys130 are now disulfide-bonded and Cys44 is unpaired. The mutant proteins are severely deficient in the catalysis of DsbA oxidation *in vitro*. These results confirm that, in the wild-type situation, UQ transition is not constitutive but induced by the reduced Cys44 residue. It is suggested that the short cytosolic loop is important for the functional turnover of DsbB cysteines and bound UQ molecules.

MATERIALS AND METHODS

Preparations of DsbB, DsbA, and their derivatives

All the DsbB constructs used in this work had their nonessential cysteines, Cys8 and Cys49, mutated to alanine and valine, respectively. They also contained a His_6-tag at the C-terminus following a factor Xa recognizable sequence, Leu–Phe–Gly–Arg. Designed mutations were introduced using QuikChange mutagenesis kit (Stratagene, La Jolla, CA) with appropriate sets of primers. DsbB-T had an insertion of Val–Pro–Arg–Gly–Ser after Leu69 to create a thrombin-recognition sequence (Leu–Val–Pro–Arg–Gly–Ser). DsbB-X had a substitution of a Factor Xa-cleavage site (Ile–Glu–Gly) for Trp67–Pro68–Leu69. DsbB proteins were overproduced and purified as described previously (7). The quinone-free form of DsbB-T (DsbB-T (ΔQ)) was prepared by expressing it in the *ubiA menA* double mutant strain (AN384) as described by Inaba *et al*. (7, 8). DsbA and its variant DsbA (C33S) were purified as described previously (7). The reduced form of DsbA was prepared as described previously (7).

Redox analyses of proteins

In vivo redox states of DsbA and DsbB were examined by growing plasmid-bearing *E. coli* strain SS141 (*dsbB*::*kan5*) (12) at 37°C in L-broth supplemented with appropriate antibiotics, 0.4% glucose and 1 m*M* isopropyl-β-D-thiogalactopyranoside (IPTG), precipitating whole proteins of the culture with trichloroacetic acid (TCA), alkylating the acid-denatured proteins in sodium dodecyl sulfate (SDS) with 4-acetamido-4'-maleimidylstilbene-2,2'-disulfonate (AMS), and detecting SDS-polyacrylamide gel electrophoresis (SDS-PAGE)-separated proteins by immunoblotting (14). The AMS-derivatized (and hence mobility-shifted) portion represented the originally reduced fraction of the protein.

Redox states of purified DsbB and DsbA were similarly determined, except that final detection was by staining with Coomassie brilliant blue (7). DsbB activity to oxidize DsbA was monitored in the presence of 200 μ*M* ubiquinone-1 (UQ1), as described (7). Reaction on ice in 50 m*M* Na-phosphate buffer (pH 8.0) containing 0.1 *M* NaCl and 0.02% n-dodecyl-β-D-maltoside (DDM) was started by mixing DsbB and reduced DsbA at a 1:1 molar ratio.

The intramolecular disulfide bridge formed between Cys41 and Cys130 of DsbB-T was determined by thrombin cleavage in combination with thiol modifications and mass analyses. DsbB-T (14 μg) was first treated with factor Xa (Novagen, Merk KGaA, Darmstadt, Germany) to cleave off the His_6-tag and then passed through Xarrest Agarose (Novagen) to remove the protease. A sample was incubated with 10 m*M* iodoacetamide (IAM) at 20°C for 5 h to block any reactive Cys residues (first modification) followed by cleavage with thrombin (2.5 units) at 20°C for 14 h. The reaction products were then reduced with dithiothreitol (DTT) (50 m*M*) at 20°C for 1 h and TCA-precipitated. The precipitates were finally dissolved in 1% SDS (buffered to pH 7.0) containing either IAM (10 m*M*) or AMS (1 m*M*), followed by incubation at room temperature for 20 min for the second cysteine modification.

Spectroscopic measurements

Absorption spectra of various DsbB preparations in 50 m*M* Na-phosphate (pH 8.0)–0.1 *M* NaCl–0.02% DDM were recorded from 300 to 700 nm using a Hitachi U-3310 spectrophotometer. DsbB activities to oxidize DsbA in the presence of UQ were assayed by monitoring fluorescence intensity changes of DsbA using a Hitachi F-4500 fluorescence spectrophotometer (2, 6). Reaction between 10 μ*M* reduced

DsbA and 10 or 200 n*M* DsbB was allowed to proceed at 30°C in 50 m*M* Na-phosphate buffer (pH 8.0) containing 0.1 *M* NaCl, 0.02% DDM, and 10 μ*M* UQ1. DsbB activities were also assayed by following DsbA-dependent reduction of UQ1 spectrophotometrically (3) at 30°C in Na-phosphate buffer (pH 8.0) containing 0.1 *M* NaCl, 0.1% DDM, UQ1, DsbB, and reduced DsbA. The reaction rate (n*M* reduced UQ1/n*M* DsbB/sec) was calculated from the initial linear absorbance decrease using an extinction coefficient difference between oxidized and reduced forms of UQ1 ($\Delta\epsilon_{275} = 12.25$).

RESULTS

DsbB-T, a DsbB variant having 5-residue insertion in the cytosolic loop, has lowered catalytic activity in vitro

DsbB contains three predicted cytosolic regions; the N-terminal tail of ~13 residues, the central loop of ~6 residues and the C-terminal tail of ~14 residues (Fig. 1a). It is unknown whether any of these short regions is functionally important. We introduced a five-amino acid insertion into the short cytosolic loop to create a thrombin cleavage site (Fig. 1a), with the original purpose of facilitating protein-chemical characterization of some intermediate states of DsbB. The variant protein, named DsbB-T, was oxidized and functional *in vivo*, since its overproduction in the Δ*dsbB* strain supported full oxidation of DsbA (data not shown).

We then solubilized DsbB-T with nonionic detergent and purified it. Its *in vitro* activity to oxidize DsbA was examined by following fluorescence changes of the latter, which exhibits increased fluorescence in the reduced state (2). While reduced DsbA (10 μ*M*) was rapidly oxidized by the UQ-coupled catalytic activity of wild-type DsbB (10 n*M*; Fig. 1b, curve D), the same concentration of DsbB-T was virtually inactive (Fig. 1b, curve A). When increased concentration (200 n*M*) of DsbB-T was used, very slow oxidation of DsbA was observed (Fig. 1b, curve C). Stoichiometric (equimolar) reaction between DsbB-T and reduced DsbA, in the presence of UQ, was also followed by the AMS modification assay (7). During this reaction, DsbA was only slowly oxidized, taking about 5 min, during which disulfide-linked DsbA–DsbB complex was observed to a small extent (Fig. 1c). The rate of this oxidation reaction was much slower than that catalyzed by the wild-type DsbB, which completed DsbA oxidation within ~10 sec under the same reaction conditions (7; data not shown). These results show that DsbB-T lacks the normal catalytic activity.

Purified DsbB-T contains only one disulfide bond

Unexpectedly, DsbB-T preparation used in the above experiment was found mostly in its partially reduced form (Fig. 1c, time 0; Fig. 2a). During the incubation with UQ and DsbA it largely remained in this partially reduced state. We also examined *in vivo* redox state of DsbB-T and found that it was mostly in the oxidized state (Fig. 2a, lane 6), being consistent with its ability to complement the chromosomal *dsbB* deletion. Apparently, DsbB-T underwent partial reduction during the course of purification.

DsbB-T exhibits constitutive ubiquinone red shift in vitro

The purified DsbB-T preparation was found to be pinkish, exhibiting marked absorbance peak at 500 nm (Fig. 2b, broken line). This absorbance curve was very similar to that exhibited by the disulfide-bonded complex between DsbB and DsbA (C33S) reported previously (7). In contrast to DsbB-T, wild-type DsbB did not itself exhibit appreciable absorption peak at 500 nm (Fig. 2b, continuous line). We also expressed DsbB-T in the *ubiA menA* double mutant strain incapable of synthesizing quinones. Spectroscopically, this preparation, DsbB-T (ΔQ), did not contain the 500 nm absorbance component (Fig. 2b, dotted line), indicating that bound quinone was responsible for the color development. Our previous studies show that the spectroscopic transition (red shift) of quinones on DsbB is induced whenever its Cys44 residue becomes unpaired and reduced. Cys44 is essential also for the DsbB-T color development because a Cys44Ser substitution abolished it (Fig. 2c, thin broken line). Importance of the Cys44 thiol in the UQ transition in DsbB-T was also indicated by the fact that IAM, a covalent thiol modifier, abolished the 500 nm absorption peak of DsbB-T (data not shown; 7). In addition, color development of DsbB-T exhibited the pH dependence that gave an apparent pK_a value, 6.4 ± 0.1, for the transition, essentially identical to the value determined with UQ bound DsbB–DsbA (C33S) complex (7). These results suggest that the color development of DsbB-T had the same chemical ground as the transient UQ transition that we described for the wild-type DsbB that is reacting with DsbA (7).

Although wild-type DsbB did not evidently show the constitutive UQ red shift, its [SCCC] and [CCSC] derivatives did so without involvement of DsbA (C33S); the former lost the Cys44 partner and the latter presumably contained the rearranged Cys41–Cys130 disulfide that results in the unpaired Cys44. In agreement with these observations, the [SCCC] and [CCSC] derivatives of DsbB-T remained red-shifted (Fig. 2c, thin and thick continuous lines, respectively); as noted previously (7), the absence of Cys41 slightly blue-shifted the peak wavelength.

When DsbB was first reduced and then incubated with UQ1, it was converted immediately into the fully oxidized form (Fig. 2d, lane 2). In this reaction, UQ1 should oxidize directly the Cys41–Cys44 pair, which in turn equilibrates with the other pair of cysteines (6, 14, 16). In contrast, UQ1 was able to oxidize the reduced form of DsbB-T only into a partially oxidized form within a few minutes (Fig. 2d, lanes 6 and 7). Its full oxidation was observed only to a limited extent, even after 30 min incubation (Fig. 2d, lane 8). These results suggest that DsbB-T has a defect in intramolecular redox communication between the N-terminal and the C-terminal pairs of cysteines.

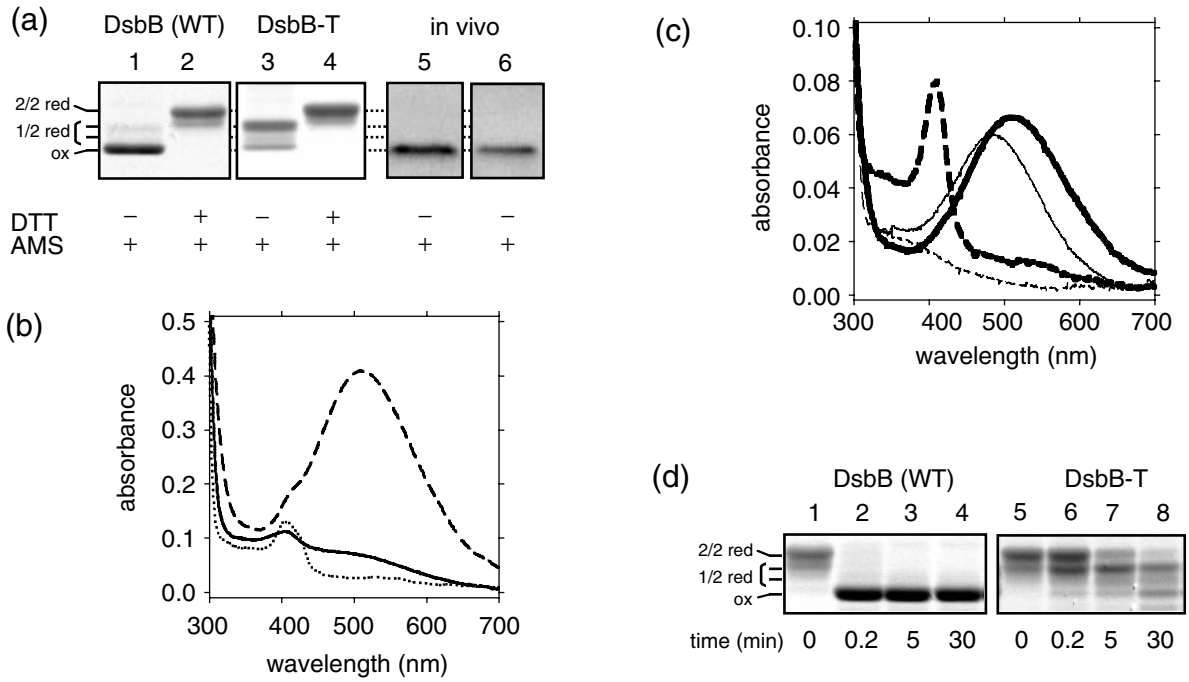

FIG. 2. Redox and spectroscopic properties of DsbB-T after purification. (**a**) Redox states of wild-type DsbB and DsbB-T. Purified preparations (10 μ*M*) of wild-type DsbB (*lanes 1 and 2*) and DsbB-T (*lanes 3 and 4*), first reduced with 100 m*M* DTT (*lanes 2 and 4*) or not (*lanes 1 and 3*), were then subjected to TCA precipitation, AMS modification, and SDS-PAGE under nonreducing conditions. *In vivo* redox states of DsbB-His_6-Myc (*lane 5*) and DsbB-T-His_6-Myc (*lane 6*) were also determined as described in Materials and Methods. (**b**) Constitutive UQ transition in DsbB-T. Absorption spectra of DsbB, DsbB-T, and DsbB-T (ΔQ) (87 μ*M* at pH 8.0) are shown in *solid*, *broken*, and *dotted lines*, respectively. (**c**) Effects of cysteine mutations on the UQ red shift of DsbB-T. Absorption spectra were recorded for 11.5 μ*M* of DsbB-T [SCCC] (*thin continuous curve*), DsbB-T [CSCC] (*thin broken curve*), DsbB-T [CCSC] (*thick continuous curve*), and DsbB-T [CCCS] (*thick broken curve*). A 400-nm peak observed for DsbB-T [CCCS] was probably due to contaminating cytochromes (1). (**d**) DsbB-T oxidation by UQ1 is incomplete. DsbB (*lanes 1–4*) and DsbB-T (*lanes 5–8*) were reduced with DTT (*lanes 1 and 5*) and then incubated with UQ1 for 10 sec (*lanes 2 and 6*), 5 min (*lanes 3 and 7*) and 30 min (*lanes 4 and 8*) at room temperature in 50 m*M* Na-phosphate (pH 8.0)–0.1*M* NaCl–0.02% DDM. Concentrations of DsbB/DsbB-T and UQ1 were 10 and 100 μ*M*, respectively. The procedures used for preparation of reduced DsbA were followed for preparation of reduced DsbB/DsbB-T, in which some air oxidation took place during the final gel filtration step, as noted previously (8).

DsbB-T contains a rearranged Cys41–Cys130 disulfide bond that unpairs Cys44

In view of the observations that purified DsbB-T was partially reduced and that it exhibited the constitutive UQ red shift, it is most likely that Cys44 is reduced in DsbB-T. A simple scenario might be that the Cys41–Cys44 disulfide was reduced due to the insertion mutation, leaving the Cys104–Cys130 disulfide unbroken. Alternatively, disulfide rearrangement might have been induced by the insertion such that an alternative combination of cysteines, Cys41 and Cys130, are now disulfide-bonded, rendering Cys44 and Cys104 reduced (7, 10). Our mutation analysis supported the latter possibility; it was found that the constitutive UQ red shift of DsbB-T was abolished not only by the Cys44Ser substitution but also by a Cys130Ser substitution (Fig. 2c, thick broken line). In the absence of Cys130, Cys44 will remain disulfide bonded with Cys41, because it will never be attacked by Cys130.

To characterize DsbB-T further, we subjected it to the following sequential manipulations: (a) blocking of free thiols with IAM; (b) cleavage with thrombin; (c) reduction with DTT of the disulfides that were originally present; and (d) AMS or IAM modification of the originally disulfide-engaged cysteines that are now reduced. The first IAM treatment (first modification) was included to avoid unwanted thiol-related reactions during the manipulations. Thrombin cleavage did not significantly alter the SDS-PAGE profile of DsbB-T under nonreducing conditions (Fig. 3a, lane 2). However, subsequent treatment with DTT split the protein into two smaller fragments (Fig. 3a, lane 3; IAM-C and IAM-N), indicating that these fragments had been held together with a disulfide bond, probably Cys41–Cys130. The sizes of the reduced fragments are consistent with their being the C-terminal (larger fragment) and the N-terminal (smaller fragment) thrombin cleavage products of DsbB-T. The electrophoretic mobilities of both fragments were upshifted when they were treated with AMS of 510 Da (Fig. 3a, lane 4) as compared

with those treated with IAM of 58 Da (Fig. 3a, lane 3). Thus, each of the fragments contained a thiol that must have been created upon reduction of the original disulfide bond. These results substantiate that the two halves of DsbB-T were disulfide-linked.

The DsbB-T fragments observed in the Fig. 3a experiment were characterized further by Peptide Mass Fingerprinting (PMF) analyses. Materials at the IAM-N, AMS-N, IAM-C, and AMS-C bands (Fig. 3a) were extracted, digested with trypsin, and subjected to matrix-assisted laser desorption ionization-time of flight (MALDI-TOF) analysis (Fig. 3c). DsbB-T-related peptides are compiled in Table 1. Among others, we observed peptides Tyr71–Arg83 of 1,634.8 Da, Phe110–Lys118 of 1,145 Da, and Asp172–Arg176 of 607.3 Da, commonly for IAM-C and AMS-C. It is notable that IAM-C gave a peak of 1,720.8 Da that corresponds to

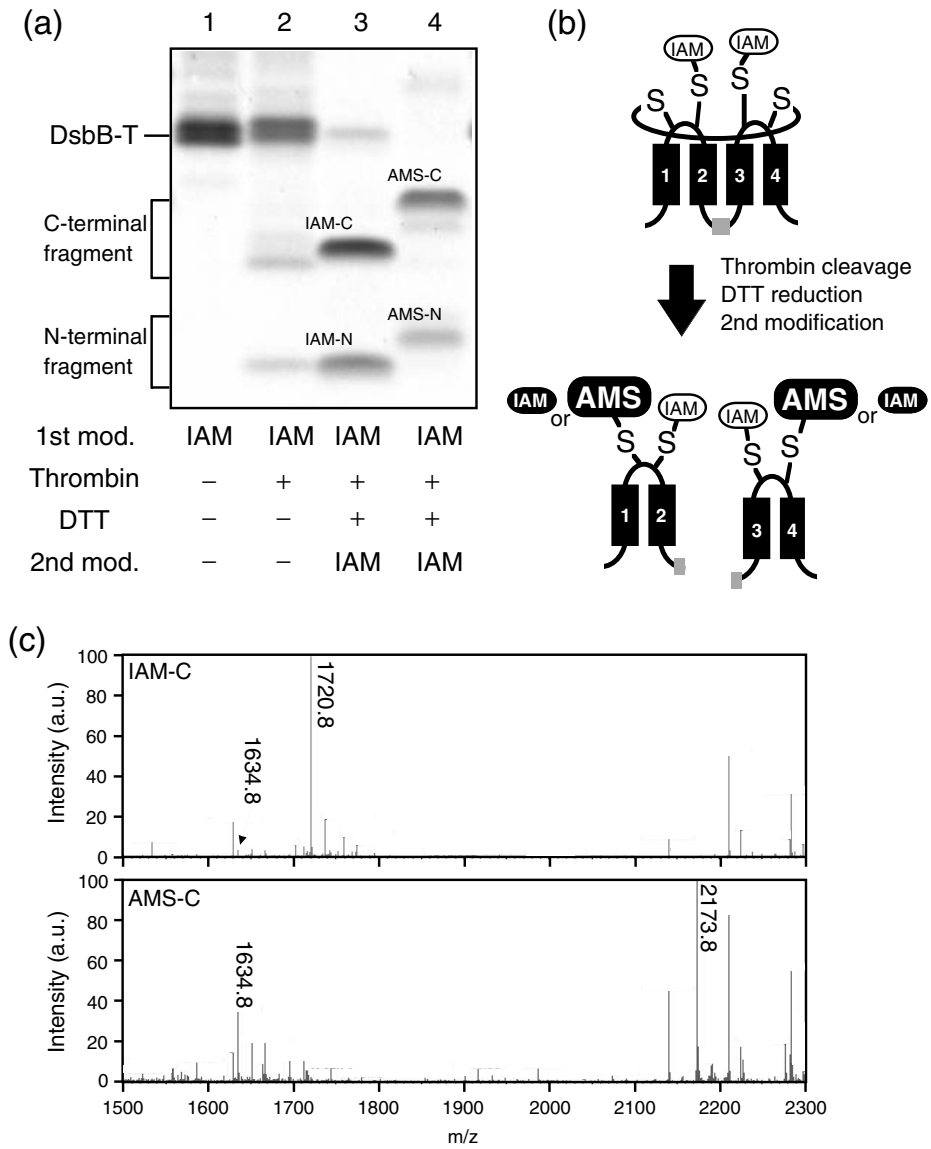

FIG. 3. Purified DsbB-T contains the Cys41–Cys130 intramolecular and interdomain disulfide bond. (**a**) SDS-PAGE patterns after sample manipulations. Purified DsbB-T (200 μl of 25 μ*M* solution) was pretreated with 10 m*M* IAM to block free cysteine residues (first modification). Subsequently, the sample was divided into four portions, which were subjected to different treatments. The first portion was directly examined without any additional treatment (*lane 1*). The second portion was treated with thrombin (*lane 2*). The remaining two portions were first reduced with DTT and then subjected to the second cysteine modification with IAM (*lane 3*) or AMS (*lane 4*). (**b**) Schematic illustrations of the products expected for *lanes 3* and *4* in (**a**). The second modifications of the cysteines originally engaged in the interdomain disulfide bond are indicated by either AMS or IAM in reverse. Transmembrane segments are numbered and the introduced thrombin recognition sequence is indicated by a *gray box*. (**c**) PMF analyses of the DsbB-T fragments. The bands IAM-C and AMS-C in (**a**) were excised and subjected to PMF. Numbers indicate molecular masses.

TABLE 1. PMF IDENTIFICATION OF THE DISULFIDE BOND THAT HAD TETHERED THE THROMBIN CLEAVAGE PRODUCTS OF DSBB-T

*Peptide**	*Modifications assigned from mass value†*	*Mass observed (Da)*	
		IAM-modified	*AMS-modified*
N-terminal fragments			
Phe4–Arg12	—	1020.5	1020.5
Val49–Lys66	—	1681.0	1681.0
Trp67–Leu69–Val–Pro–Arg‡	—	682.4	682.4
C-terminal fragments			
Tyr71–Arg83	Met74	1634.8	1634.8
Gly84–Arg109	Met93/107, Cys104	3136.4	Not detected
Phe110–Lys118	—	1144.6	1144.5
Trp119–Arg133	—	1720.8	2173.8
Asp172–Arg176	Cys130	607.3	607.3

*Residue numbers are those for wild-type DsbB protein.

†Modified amino acid residues that are consistent with the measured mass are indicated. An oxidized methionine increases the peptide mass by 16 Da.

‡This peptide includes a part of the mutationally inserted amino acids, which are not numbered.

Phe119–Arg133 that was modified with IAM, but this peak was absent from the AMS-C sample. Instead, AMS-C gave a new peak at molecular mass of 2,173.8 Da (Fig. 3c), consistent with that of AMS-modified Phe119–Arg133. We conclude that these peaks represent Phe119–Arg133, whose Cys130 had been modified either with IAM or AMS in the course of the second modification reactions. It is thus clear that Cys130 but not Cys104 was originally engaged in the intramolecular disulfide bond formation. We believe that the disulfide bond partner of Cys130 is Cys41, for the following reasons. First, the UQ transition on DsbB-T means that its Cys44 must be reduced. Secondly, Kadokura and Beckwith (10) showed that a split DsbB can be held together by the Cys41–Cys130, but not Cys44–Cys130, disulfide bond. The PMF experiments did not reveal an expected Pro40–Glu48 fragment with modified Cys44, presumably due to the low recovery of the modified peptides (8).

The short cytosolic loop tunes DsbB-quinone complex to enable its proper turnover

The partial reduction and the constitutive quinone transition can either be properties specific for the inserted amino acid sequence in DsbB-T or be due to disruption of the intrinsic structural/functional role that the cytosolic loop possesses naturally. To clarify this point, we constructed several other variants with an altered loop region. DsbB-X was a variant, in which the Trp67–Pro68–Leu69 segment was replaced by Ile–Glu–Gly, generating a Factor Xa-cleavage site. After purification, DsbB-X proved to exist mainly as the hemireduced form (Fig. 4b, lane 3) and to exhibit an evident absorbance peak at 500 nm (Fig. 4a, second curve). We also constructed and purified DsbB variants having one of single amino acid substitutions, Thr67Ala, Pro68Ala, and Leu69Ala, as well as

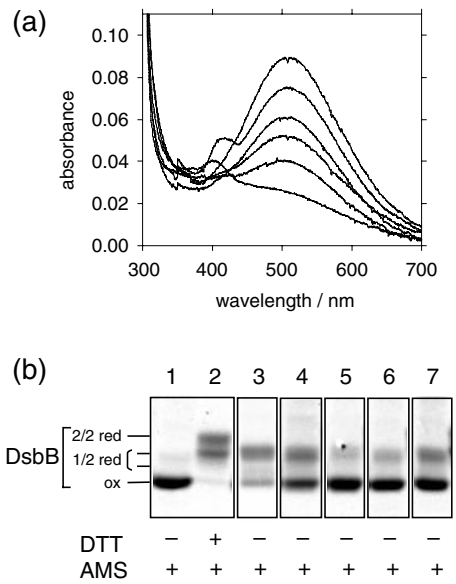

FIG. 4. Alterations of the cytosolic loop result in partial reduction of DsbB, in which UQ transition is induced. (**a**) Absorbance spectra of the DsbB derivatives. Absorbance was scanned at pH 8.0 for 20 μ*M* solutions of DsbB (T67A), DsbB-X, DsbB (70A), DsbB (L69A), DsbB (P68A), and wild-type DsbB (from upper to lower peaks at ~500 nm). A minor peak at 400 nm for DsbB-X was presumably due to contaminating cytochromes. (**b**) Redox states of the DsbB derivatives after purification. Preparations of DsbB (*lanes 1 and 2*), DsbB-X (*lane 3*), DsbB (T67A) (*lane 4*), DsbB (P68A) (*lane 5*), DsbB (L69A) (*lane 6*), and DsbB (70A) (*lane 7*) were subjected to TCA precipitation, AMS modification, and SDS-PAGE. The *lane 2* sample had been reduced with DTT before examination. Shown are Coomassie brilliant blue-stained patterns.

Table 2. DsbA Oxidation Activities of DsbB Variants with an Altered Cytosolic Loop

DsbB	*Rate of DsbA oxidation (nM DsbA/nM DsbB/sec)*
Wild type	5.4
DsbB-T	2.0×10^{-1}
DsbB-X	3.4×10^{-2}
DsbB(T67A)	4.4×10^{-1}
DsbB(P68A)	1.9
DsbB(L69A)	9.1×10^{-1}
DsbB(70A)	2.1×10^{-1}

DsbB activity was actually assayed by the DsbA-dependent reduction of UQ (see Materials and Methods).

one with a single alanine insertion after Leu69, named DsbB (70A). All of them were in their hemireduced forms to significant extents (Fig. 4b, lanes 4–7). Also, they all had an absorbance peak at 500 nm (Fig. 4a). Finally, they all had markedly reduced levels of *in vitro* catalytic activities to oxidize DsbA (Table 2), ranging from 0.6% (DsbB-X) to 35% (DsbB (P68A)) of the wild-type activity. Rough correlations were observed between the extents of the 500 nm absorption and the extents of activity impairments. It seems that static UQ transition is deleterious for the catalytic turn over of the DsbB–UQ complex. However, activities of the DsbB mutants were lower than what could be expected if the fully oxidized fractions retained full activity (Fig. 4b and Table 2). Thus, the mutations compromised the catalytic function of DsbB regardless of its initial oxidation state.

These results show that not only the five amino acid insertion in DsbB-T but also other sequence alterations, including single alanine substitutions in the central cytosolic region of DsbB, result in the partial reduction, constitutive transition of bound UQ, and lowered activity. Thus, the cytosolic loop of DsbB does not solely function to maintain the membrane-integrated state of DsbB. It has an active role in coordinating the reactivities of the cysteine-containing active sites of DsbB such that they can facilitate continuous electron flow, in which bound quinone molecules turn over effectively.

DISCUSSION

Our previous studies using DsbB preparations that bore UQ (7), that bore menaquinone (19) and that were free of endogenous quinones (8) showed that the DsbB-mediated oxidation of DsbA proceeds via either of two reaction pathways, rapid and slow. In the rapid pathway, dithiol–disulfide exchange takes place directly between the Cys30–Cys33 residues of DsbA and the Cys104–Cys130 disulfide of DsbB. This is then followed by rapid equilibrium of now reduced Cys104–Cys130 pair and the Cys41–Cys44 disulfide within DsbB, which is driven by quinone-dependent oxidation of the Cys41 and Cys44 pair to produce the oxidized forms of both DsbA and DsbB. In the slow pathway, the disulfide-bonded DsbA (Cys30)–DsbB (Cys104) complex is formed as a transient but considerably stable intermediate, in which intramolecular disulfide rearrangement occurs such that Cys41 is now disulfide-bonded with Cys130. A remarkable feature of the latter pathway is that the unpaired Cys44 induces spectroscopic transition (red shift) of bound quinone molecules, thus exhibiting an absorption maximum at 500 nm (in the case of UQ) or at 550 nm (in the case of menaquinone). Evidence suggests that in the intermediate, quinone forms a charge transfer complex with the Cys44 thiolate anion (8a). The rapid pathway reaction might also involve the quinone transition state albeit extremely short-lived (19).

Although Regeimbal *et al*. (17) also reported similar spectroscopic properties of DsbB-bound UQ, there is an important difference between our observation and that of Regeimbal *et al*. While Regeimbal *et al*. observed the absorption change of UQ in their DsbB samples prepared at high pH, in our case DsbB by itself does not evidently exhibit the UQ red shift. Instead, extensive UQ transition occurs transiently when DsbB is catalyzing DsbA oxidation or stably when it is complexed with DsbA (C33S), a DsbA variant that forms the intermediate-like covalent and stable heterodimer. Our present results of the mutational induction of the UQ red shift rend further support to the notion that the UQ red shift is not a constitutive property for wild-type DsbB enzyme *per se*. However, as our analyses show that UQ red shift occurs whenever Cys44 of DsbB gets reduced (7), it is possible that even wild-type DsbB may be able to assume, under certain experimental conditions (17), a state in which UQ is red-shifted. Closer examinations of our preparations of wild-type DsbB did reveal variable and very small A_{500} peaks. In any case, the probability of UQ red shift (hence reduction of Cys44) must be small for wild-type DsbB.

Our present results indicate that the probability of the Cys44 reduction is increased by the five-residue insertion into the cytosolic loop in DsbB-T. Although DsbB-T was oxidized and sufficiently functional *in vivo*, it is transformed into a partially reduced form after detergent solubilization and purification. The purified DsbB-T was pink-colored; it exhibited constitutive induction of UQ transition without involving the mixed disulfide formation with DsbA. By combined two-step cysteine modifications, thrombin cleavage, and mass spectrometric analyses, we have shown that the DsbB-T preparation contains the Cys41–Cys130 interloop disulfide bond, whereas its Cys44 is now reduced. Kadokura and Beckwith (10) first proposed and demonstrated using split DsbB constructions that DsbA–DsbB interaction led to the formation of the intermediate complex having two disulfide bonds between Cys30 (DsbA) and Cys104 (DsbB) as well as between Cys41 and Cys130 within DsbB. We showed that Cys41 and Cys130 in a DsbB variant, DsbB [CSSC], form an intramolecular disulfide bond (7). Taken together with the results reported here, it is likely that Cys41 and Cys130 are located in close mutual proximity in the three-dimensional structure of DsbB. Since this alternative cysteine pair has a redox potential value that is similar to those of Cys41–Cys44 and Cys104–Cys130 pairs (8), it could form a disulfide depending on factors such as availability of Cys130 as the nucleophilic attacker

as well as by subtle change in the free energy states of the different disulfide bonds in this system.

Our analyses indicate that DsbB-T has features characteristic of the slow pathway intermediate in that it contains the rearranged Cys41–Cys130 disulfide, reduced Cys44, and red-shifted UQ. However, DsbB-T has an essential difference from the intermediate in that it does not bear any DsbA molecule. In fact, the formation of such a structure prematurely without involving the reaction partner, DsbA, seems to be deleterious to the functioning of DsbB, and DsbB-T had greatly diminished DsbA oxidation activity *in vitro*. Similar partial reduction, constitutive UQ red shift, and compromised functionality were manifested to different extents by other alterations of the short cytosolic loop, including single alanine substitutions and a single alanine insertion into this region. Thus, the integrity of this cytosolic region is required for the normal reactivities of active site cysteines on the periplasmic side of DsbB.

One possible mechanism of the mutational effects might be that the mutations alter the redox potentials of the Cys41–Cys44, Cys104–Cys130 and/or Cys41–Cys130 pairs, for instance to stabilize the rearranged Cys41–Cys130 disulfide bond. However, our determinations using [SSCC] and [CSSC] variants of DsbB-T and DTT redox buffers did not reveal changes in this direction; the redox potential values of both Cys104–Cys130 and Cys41–Cys130 were a couple of dozen millivolts higher in the DsbB-T mutant than in wild-type DsbB (Y-H Takahashi, unpublished results). Although we were unable to determine the redox potential of Cys41–Cys44 in DsbB-T [CCSS] because this variant protein was unstable and prone to aggregation, we determined that of Cys41–Cys44 in DsbB-X [CCSS] to be about -215 mV, not significantly deviating from the wild-type value (Y-H. Takahashi, unpublished results). Thus, it is unlikely that the effects of the cytosolic alterations were brought about by redox potential changes of any cysteine combination. It should be noted that the above approaches of using cysteine mutations have limitations because it is the interaction between different sets of cysteines that should be examined. In any case, the formation of the Cys41–Cys130 disulfide bond in expense of the reduction of Cys44 in DsbB-T indicates that the cytosolic loop has a role of properly adjusting the relative stabilities among the three known combinations of cysteine pairs that the four essential cysteines can form intramolecularly.

The DsbB-T preparation that carries the already formed Cys41–Cys130 interloop disulfide bond is inactive in DsbA oxidation. This form of DsbB-T was never oxidized further, even by a strong oxidant such as potassium ferricyanide (Y-H. Takahashi, unpublished results). Thus, Cys44 and Cys104 seem to be located distantly from each other in the tertiary structure of DsbB. Thus, if all the four essential cysteines are to be engaged in disulfide bonds, the only possible combination is the "normal" combination. In other words, full oxidation of DsbB means exclusively the state in which disulfide bonds are formed in the combinations of Cys41–Cys44 and Cys104–Cys130. When DsbB-T had once been reduced fully with DTT, it was now fully oxidized by ferricyanide, without restoring the catalytic DsbA-oxidizing activity (Y-H Takahashi, unpublished results). These results indicate that DsbB-T lacks the full catalytic activity not only in the trapped partially reduced form but also in its fully oxidized form. However, it should be more accurate to state that DsbB-T will anyway end up with nonproductive states during the reaction cycle, irrespective of the initial redox states. Even if it could engage in limited and stoichiometric disulfide–dithiol exchange reaction under certain experimental settings, it cannot turn over effectively. In fact, unlike the nonspecific ferricyanide, the physiological oxidant, UQ, was only able to oxidize one pair of the DsbB-T cysteines with reasonable rapidity (Fig. 2d). In the wild-type situation, UQ-dependent oxidation of Cys41 and Cy44 is rapidly equilibrates within DsbB (6, 16). DsbB-T seems to have defects in the intramolecular transmission of the UQ-originated oxidizing equivalents.

The robust inability of the Cys41–Cys130 tethered DsbB-T to undergo further disulfide rearrangement raises a question of why the real intermediate can be resolved into the oxidized forms of DsbA and DsbB coupled with reduction of quinone. The fact that mutating Cys33 of DsbA can also generate a dead-end state suggests that this DsbA residue participates in the resolution of the physiological intermediate. Our results show that, in the absence of DsbA, the Cys44–UQ charge-transfer complex cannot complete two-electron transfer to UQ that is accompanied by the resolution of Cys41–Cys130 and the formation of the two disulfide bonds. Sevier *et al*. (18) proposed that DsbB and its eukaryotic functional homologues, Ero1p and Erv2p, share some structural features, one of which is the flexibility of a loop containing one of the redox-active cysteine pairs of these proteins. Its equivalent in DsbB, the second periplasmic loop, may be recognized specifically by DsbA, leading to some conformational change of the loop. We suggest that such specific DsbA–DsbB interaction not only enables the initiation of the rapid pathway reaction (8), but also enables the resolution process of the slow pathway reaction. The resolution of the Cys41–Cys130 disulfide should require coordinated actions of the Cys44–UQ charge transfer complex and Cys33 of DsbA, and this process may only be possible after the establishment of the specific DsbA–DsbB association.

We have shown here that not only the insertion mutations but also more subtle single amino acid substitutions in the cytosolic loop affected the DsbB functionality at least *in vitro*. However, when these DsbB variants were overproduced in the Δ*dsbB* strain, all of them complemented the defect of the Δ*dsbB* cells to maintain DsbA oxidized (data not shown). Kadokura and Beckwith (10) even split DsbB at this region and showed that the split DsbB was still functional *in vivo*. It is possible that membrane integration and overproduction have helped the DsbB variants to interact productively with DsbA and with quinones. Alternatively or in addition, the membrane integration may stabilize the native structures of the DsbB variants. It should be noted, however, that the detergent–solubilized DsbB variants still retained the native-like structure, at least to the extent that they interacted with UQ to induce the spectral transition. At any rate, our *in vitro* results suggest that the short cytosolic loop contributes to the stability and functionality of DsbB, as well as to the prevention of the premature formation of Cys41–Cys130 before establishment of proper interaction with DsbA. This loop may coordinate the reactivities of the cysteine-containing active site domains of DsbB such that they can cooperatively facilitate the continuous electron flow, in which bound quinone molecules turn over effectively.

ACKNOWLEDGMENTS

The authors thank Hiroyuki Mori and Yoshinori Akiyama for stimulating discussion. We are also grateful to Junko Moriwaki-Hattori and Kiyoko Mochizuki for technical supports. This work was supported by grants from CREST, Japan Science and Technology Agency, from the Ministry of Education, Culture, Sports, Science and Technology, Japan, and its National Project on Protein Structural and Functional Analyses.

ABBREVIATIONS

AMS, 4-acetamido-4'-maleimidylstilbene-2,2'-disulfonate; DDM, n-dodecyl-β D-maltoside; DTT, dithiothreitol; IAM, iodoacetamide; IPTG, isopropyl-β-D-thiogalactopyranoside; MALDI–TOF, matrix-assisted laser desorption ionization-time of flight; PAGE, polyacrylamide gel electrophoresis; PMF, peptide mass fingerprinting; SDS, sodium dodecyl sulfate; TCA, trichloroacetic acid; UQ, ubiquinone; UQ1, ubiquinone-1 (a commercial chemical product used as an exogenous source of ubiquinone *in vitro*). Four letter (C or S) notations after DsbB specify whether the essential cysteines, at positions 41, 44, 104, and 130, remain unaltered (C) or mutated to serine (S).

REFERENCES

1. Bader M, Muse W, Ballou, DP, Gassner C, and Bardwell JCA. Oxidative protein folding is driven by the electron transport system. *Cell* 98: 217–221, 1999.
2. Bader M, Muse W, Zander T, and Bardwell J. Reconstitution of a protein disulfide catalytic system. *J Biol Chem* 273: 10302–10307, 1998.
3. Bader M, Xie T, Yu C-A, and Bardwell JCA. Disulfide bonds are generated by quinone reduction. *J Biol Chem* 275: 26082–26088, 2000.
4. Grauschopf U, Fritz A, and Glockshuber R. Mechanism of the electron transfer catalyst DsbB from *Escherichia coli*. *EMBO J* 22: 3503–3513 2003.
5. Guilhot C, Jander G, Martin NL, and Beckwith J. Evidence that the pathway of disulfide bond formation in *Escherichia coli* involves interactions between the cysteines of DsbB and DsbA. *Proc Natl Acad Sci USA* 92: 9895–9899, 1995.
6. Inaba K and Ito K. Paradoxical redox properties of DsbB and DsbA in the protein disulfide-introducing reaction cascade. *EMBO J* 21: 2646–2654, 2002.
7. Inaba K, Takahashi Y-h, Fujieda N, Kano K, Miyoshi H, and Ito K. DsbB elicits a red-shift of bound ubiquinone during the catalysis of DsbA oxidation. *J Biol Chem* 279: 6761–6768, 2004.
8. Inaba K, Takahashi Y-H, and Ito K. Reactivities of quinone-free DsbB from *Escherichia coli*. *J Biol Chem* 280: 33035–33044, 2005.

8a. Inaba K, Takahashi Y-H, Ito K, and Hayashi S. Critical role of a thiolate–quinone charge transfer complex and its adduct form in *de novo* disulfide bond generation by DsbB. *Proc Natl Acad Sci USA* 103: 287–292, 2006.

9. Jander G, Martin NL, and Beckwith J. Two cysteines in each periplasmic domains of the membrane protein DsbB are required for its function in protein disulfide bond formation. *EMBO J* 13: 5121–5127, 1994.
10. Kadokura H and Beckwith J. Four cysteines of the membrane protein DsbB act in concert to oxidize its substrate DsbA. *EMBO J* 21: 2354–2363, 2002.
11. Kadokura H, Katzen F, and Beckwith J. Protein disulfide bond formation in prokaryotes. *Annu Rev Biochem* 72: 111–135, 2003.
12. Kishigami S, Kanaya E, Kikuchi M, and Ito K. DsbA-DsbB interaction through their active site cysteines. Evidence from an odd cysteine mutant of DsbA. *J Biol Chem* 270: 17072–17074, 1995.
13. Kobayashi T, Kishigami S, Sone M, Inokuchi H, Mogi T, and Ito K. Respiratory chain is required to maintain oxidized states of the DsbA-DsbB disulfide bond formation system in aerobically growing *Escherichia coli*. *Proc Natl Acad Sci USA* 94: 11857–11862, 1997.
14. Kobayashi T and Ito K. Respiratory chain strongly oxidizes the CXXC motif of DsbB in the *Escherichia coli* disulfide bond formation pathway. *EMBO J* 18: 1192–1198, 1999.
15. Nakamoto H and Bardwell JCA. Catalysis of disulfide bond formation and isomerization in the *Escherichia coli* periplasm. *Biochim Biophys Acta* 1694: 111–119, 2004.
16. Regeimbal J and Bardwell JCA. DsbB catalyzes disulfide bond formation *de novo*. *J Biol Chem* 277: 32706–32713, 2002.
17. Regeimbal J, Gleiter S, Trumpower B, Yu C-A, Diwaker M, Ballou DP, and Bardwell JCA. Disulfide bond formation involves a quinhydrone-type charge-transfer complex. *Proc Natl Acad Sci USA* 100: 13779–13784, 2003.
18. Sevier CS, Kadokura H, Tam VC, Beckwith J, Fass D, and Kaiser CA. The prokaryotic enzyme DsbB may share key structural features with eukaryotic disulfide bond forming oxidoreductases. *Protein Sci* 14: 1630–1642, 2005.
19. Takahashi Y-h, Inaba K, and Ito K. Characterization of the menaquinone-dependent disulfide bond formation pathway of *Escherichia coli*. *J Biol Chem* 279: 47057–47065, 2004.

Address reprint requests to:
Koreaki Ito
Institute for Virus Research
Kyoto University
Sakyo-ku, Kyoto 606–8507, Japan

E-mail: kito@virus.kyoto-u.ac.jp

Date of first submission to ARS Central, November 5, 2005; date of acceptance, November 19, 2005.

This article has been cited by:

1. Kenji Inaba, Satoshi Murakami, Atsushi Nakagawa, Hiroka Iida, Mai Kinjo, Koreaki Ito, Mamoru Suzuki. 2009. Dynamic nature of disulphide bond formation catalysts revealed by crystal structures of DsbB. *The EMBO Journal* **28**:6, 779-791. [CrossRef]
2. A VLAMISGARDIKAS. 2008. The multiple functions of the thiol-based electron flow pathways of Escherichia coli: Eternal concepts revisited. *Biochimica et Biophysica Acta (BBA) - General Subjects* **1780**:11, 1170-1200. [CrossRef]
3. Hiroshi Kadokura . 2006. Oxidative Protein Folding: Many Different Ways to Introduce Disulfide BondsOxidative Protein Folding: Many Different Ways to Introduce Disulfide Bonds. *Antioxidants & Redox Signaling* **8**:5-6, 731-733. [Citation] [PDF] [PDF Plus]